PROCEEDINGS OF SPIE

SPIEDigitalLibrary.org/conference-proceedings-of-spie

Optical method for making spatially and temporally resolved measurements of the hole concentration in organic electrochemical transistors

Jacob T. Friedlein, Sean E. Shaheen, Robert R. McLeod

Jacob T. Friedlein, Sean E. Shaheen, Robert R. McLeod, "Optical method for making spatially and temporally resolved measurements of the hole concentration in organic electrochemical transistors," Proc. SPIE 9185, Organic Field-Effect Transistors XIII; and Organic Semiconductors in Sensors and Bioelectronics VII, 91851X (7 October 2014); doi: 10.1117/12.2063564

SPIE.

Event: SPIE Organic Photonics + Electronics, 2014, San Diego, California, United States

Downloaded From: https://www.spiedigitallibrary.org/conference-proceedings-of-spie on 6/16/2018 Terms of Use: https://www.spiedigitallibrary.org/terms-of-use

Optical method for making spatially and temporally resolved measurements of the hole concentration in organic electrochemical transistors

Jacob T. Friedlein*[a], Sean E. Shaheen[a,b,c], Robert R. McLeod[a]
[a]University of Colorado, Dept. of Electrical, Computer, and Energy Engineering, 425 UCB, Boulder, CO 80309-0425.
[b]University of Colorado, Dept. of Physics, 390 UCB, Boulder, CO 80309-0390.
[c]University of Colorado and National Renewable Energy Laboratory, 27 UCB Suite 208, Boulder, CO 80309-0027.

ABSTRACT

Electrochemical reduction and oxidation of PEDOT:PSS are used to modulate the channel current in organic electrochemical transistors (OECTs). In addition to changing PEDOT conductivity over more than 4 orders of magnitude, these redox reactions cause a shift in the PEDOT:PSS absorption spectrum. In this work we have used this shift in the absorption spectrum to make spatially and temporally resolved measurements of the redox state of PEDOT:PSS. By applying these measurements to the PEDOT:PSS in an OECT channel, we have shown that the redox state of the PEDOT:PSS is not constant along the channel during transistor operation. Furthermore, we have shown that the time constant of the optical transition is significantly larger near the transistor source than it is near the transistor drain. These results are not considered in existing models of the OECT transient response, and they may lead to a better understanding of geometry-performance relationships in OECTs.

Keywords: Organic electrochemical transistors, PEDOT:PSS, electrochromism, organic electronics, iontronics, biosensors

1. INTRODUCTION

The biocompatibility[1] and exceptional transconductance of OECTs[2] make these devices promising for a number of high sensitivity biosensing applications. For instance, they have been used *in vitro* to detect epithelial cell integrity after exposure to various toxins[3], complementary DNA strands with concentrations down to 10 pm[4], and acetylcholine concentrations[5]. Additionally, they have been used *in vivo* as bioresorbable electrocardiographic recording devices[6] and as sensors to detect epileptic activity in rat brains[7]. For such applications, both high transconductance and high speed operation are needed. Therefore, a detailed model of the transient response of an OECT is necessary in order to correctly interpret the measured signal. However, such a model does not currently exist in the literature. In this paper, we will demonstrate a method that can be used to obtain data that will inform such a model. To demonstrate this method, we will begin with an introduction about OECT operation, modeling, and characterization. Then we will discuss our methods for making spatially and temporally resolved measurements of the hole density in OECTs. And, finally, we will discuss our results obtained using this method.

1.1 OECT operation

The functional element of an OECT is a conducting channel made of poly(3,4-ethylene-dioxythiophene):poly(styrenesulfonate) (PEDOT:PSS), a highly-conductive, degenerately doped organic semiconductor. PEDOT:PSS can have conductivities greater than 1000 S/cm[8]; however, when the PEDOT is electrochemically reduced to its neutral state, according to equation (1), its conductivity can drop by more than 4 orders of magnitude.

*jacob.friedlein@colorado.edu, phone: 308-672-4896;

Organic Field-Effect Transistors XIII; and Organic Semiconductors in Sensors and Bioelectronics VII, edited by Zhenan Bao, Iain McCulloch, Ruth Shinar, Ioannis Kymissis, Proc. of SPIE Vol. 9185, 91851X · © 2014 SPIE · CCC code: 0277-786X/14/$18 · doi: 10.1117/12.2063564

Downloaded From: https://www.spiedigitallibrary.org/conference-proceedings-of-spie on 6/16/2018 Terms of Use: https://www.spiedigitallibrary.org/terms-of-use

In an OECT, equation (1) is driven to either the right or left side by the application of a positive or negative gate voltage[9]. In the OFF state, a positive gate voltage is applied, and cations drift into the PEDOT:PSS channel; whereas, in the ON state, the gate voltage is set to 0 V, and the cations are allowed to diffuse out of the channel, as shown in Fig. 1.

$$PEDOT^{+}:PSS^{-} + Na^{+} + e^{-} \rightarrow PEDOT^{0} + Na^{+}:PSS^{-} \quad (1)$$

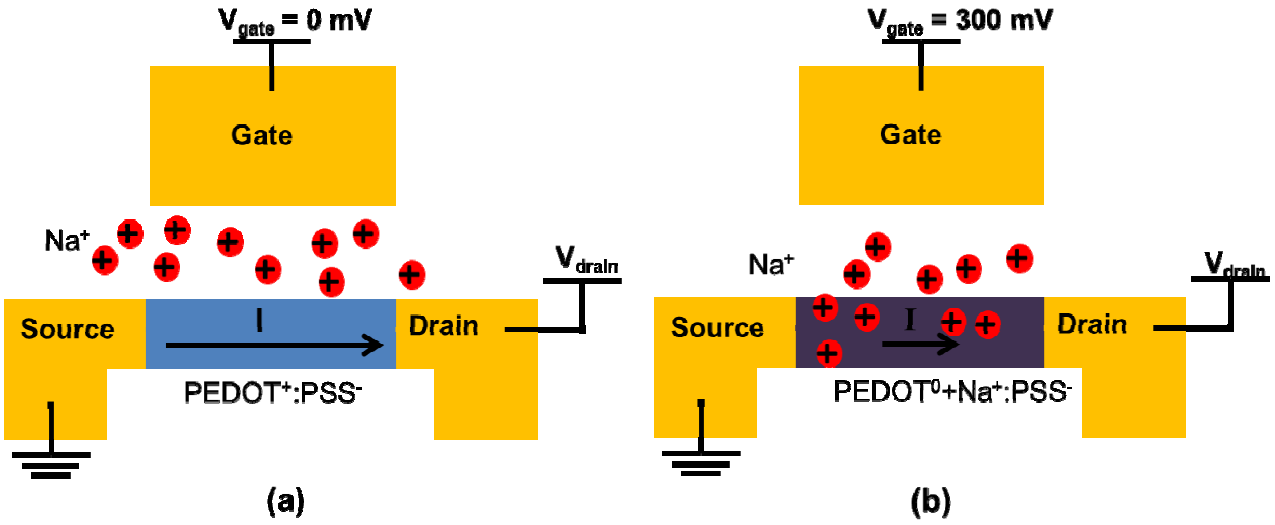

Figure 1. (a) Schematic of an OECT in the ON state. The gate voltage is at 0 V, and there are almost no cations in the OECT channel. (b) OECT in the OFF state. The gate voltage has been stepped to a positive value, and a large number of cations are in the OECT channel. The PEDOT is electrochemically reduced to its neutral state and becomes insulating.

1.2 Existing models of OECT transient response

Although several authors have shown that OECTs with shorter channels are faster than long channel devices[10,11], the OECT literature still lacks a systematic empirical study of response speed as a function of channel length. Moreover, there is a dearth of papers presenting models of the transient response of OECTs. To our knowledge, the only model of OECT transient responses was presented in the seminal paper on modeling OECTs by Bernards and Malliaras. This work points out the importance of the interplay between two time constants in OECTs[9]. The electrical time constant, which describes the amount of time it takes a hole to traverse the OECT channel, is determined by the hole mobility, channel length, and source-drain voltage. The ionic time constant describes how quickly cations can be injected into the transistor channel from the electrolyte, and it is determined by the RC time constant of the ionic circuit linking the transistor gate to the transistor channel. This model shows that there will be two regimes of operation, one in which device speed is limited by the ionic circuit and one in which it will be limited by the transit time of holes. However, because the model assumes a spatially uniform hole density along the channel, it fails to predict a response speed that depends on channel length – even in the case when the electrical time constant is larger than the ionic time constant. Other work reiterates the importance of the interplay between the electronic and ionic time constants in electrolyte-gated field effect transistors[12]. The authors of that work show that long-channel devices operate at speeds slower than the ionic time constant, and that their switching speeds vary with channel length. For devices with channels shorter than a characteristic length, the ionic time constant dominates, and the response speed no longer depends on channel length. Interestingly, even the long-channel devices do not obey the expected relationship between channel length and response time; rather, they follow a $\tau \propto L^{1.6}$ relationship instead of the expected $\tau \propto L^{2}$. Because the existing models fail to satisfactorily explain the relationship between channel length and switching speed, a better model is needed. However, before we can develop such a model, we need to better understand both spatial and temporal variations in the hole density in the OECT channel. Unfortunately, obtaining such data is difficult with electrical measurements, which cannot spatially resolve conductivity in the channel, but by capturing channel current, perform a weighted spatial averaging across the entire OECT channel.

Downloaded From: https://www.spiedigitallibrary.org/conference-proceedings-of-spie on 6/16/2018 Terms of Use: https://www.spiedigitallibrary.org/terms-of-use

1.3 Optical methods for measuring hole density in PEDOT:PSS

Because electrochemical oxidation (reduction) creates (removes) midgap polaron energy levels on the PEDOT chain, changes in oxidation state are directly related to changes in PEDOT color. As the PEDOT is oxidized, polaron levels are introduced in the HOMO-LUMO band gap; this causes both an increase in hole concentrations and a shift of the absorption spectrum peak from the red to the infrared[13]. Therefore, the optical and electrical responses of PEDOT:PSS are directly linked, and we can use optical measurements to monitor the conductivity of PEDOT:PSS[13,14]. Unlike measurements of channel current in OECTs, these optical measurements do not necessitate spatial averaging over the entire OECT channel. In fact, it has been shown that such methods can be used to track electrochemical dedoping fronts in polypyrrole:dodecylbenzenesulfonate and PEDOT:PSS films[15,16]. Furthermore, it has been shown that UV-vis-NIR spectroscopy can be used to confirm electrochemical dedoping in PEDOT:PSS-based devices[17,18]. However, in these studies, the electrochromic response was averaged over a large area, and spatial gradients in the hole density were not measured. To our knowledge, no spatially and temporally resolved studies of hole density in OECTs have been made. However, such a study is precisely what is needed in order to develop a better model for OECT transient responses. Therefore, in this work, we have measured local hole densities throughout an OECT channel during device switching, and we have demonstrated that these measurements can be used to advance our understanding of OECT transient responses.

2. METHODS

In this study, lateral OECTs were fabricated as follows: First, Cr (5 nm)/Au (100 nm) source, drain, and gate electrodes were patterned on glass substrates using thermal evaporation and standard photolithographic liftoff techniques. Next, the chip was cleaned via sonication in isopropanol and a 5 min. 150^{o} C dehydration bake in ambient conditions. Then, a PEDOT:PSS formulation was spun-cast on the chip. After baking for 10 min. at 150^{o} C in ambient conditions, the PEDOT:PSS was patterned by scratching away the polymer with a 5 μm radius tungsten probe tip controlled by a micropositioning system. After the PEDOT:PSS was patterned, a sodium-based gel electrolyte solution was drop cast over the entire chip and allowed to dry at room temperature for more than 24 hours. An image of one of the resulting devices is shown in Fig. 2.

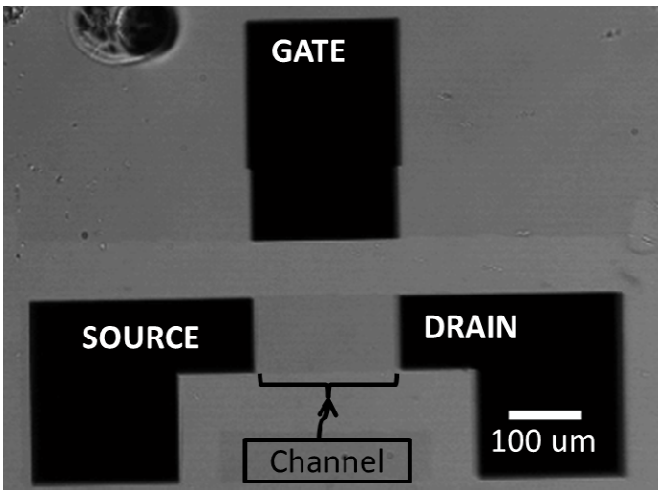

Figure 2. Optical microscope image of an OECT.

The electrical characterization of the devices was performed with a Keithley 2636A source meter unit with custom-written control code that executed a 5 ms measurement trigger model. The optical measurements were taken simultaneously with the electrical measurements. The chip was illuminated from the bottom by a ThorLabs MCWHL2 white LED, and the images were captured from above the chip through a 10x/0.25 NA objective. The camera used for the characterization was a monochrome, high-speed, global shutter CMOS sensor. After the optical measurements were made, the 8-bit images were convolved with a 5 pixel x 5 pixel Gaussian kernel with a standard deviation of 10. Because we used transmission mode illumination, and because the spectrum of the illumination source did not contain any infrared, oxidation resulted in a brightening of the captured image; whereas, reduction caused a darkening of the

Downloaded From: https://www.spiedigitallibrary.org/conference-proceedings-of-spie on 6/16/2018 Terms of Use: https://www.spiedigitallibrary.org/terms-of-use

captured image (see Fig. 3). In agreement with past studies[19], we have assumed a linear relationship between optical intensity change and change in conductivity.

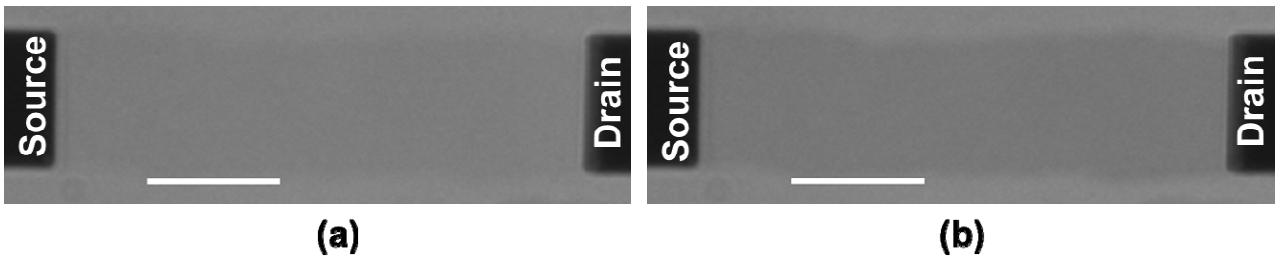

Figure 3. Unprocessed images of an OECT channel during device operation. (a) an optical microscope image with all electrodes floating. (b) an image with V_{Source} = 0 V, V_{Drain} = -300 mV, V_{Gate} = 300 mV. The gate is not in the captured frame. It is 120 μm away from the OECT. Scale bar is 50 μm.

3. RESULTS

Figure 4 shows a typical series of frames during the switching event in our OECTs. It is clear from these images that the channel changes color and reaches a steady state in less than 50 ms after the gate voltage is stepped. Furthermore, it is clear that the conductivity decrease is more intense near the drain electrode than it is near the source electrode. To emphasize this second point, we have taken a single image from the sequence of images and plotted the color change profile along the length of the channel. This result is shown in Fig. 5. Although fitting a model to these data is not within the scope of this paper, the nonlinear decrease in conductivity suggests a Poisson-Boltzmann distribution, balancing the drift and diffusion of cations in the OECT channel[20].

Not only did we use our optical data to obtain a spatial conductivity profile at a snapshot in time, we also used it to find how channel conductivity evolved with time. To obtain this result, we averaged 30 pixel columns (~ 15 μm) of the OECT channel near the drain electrode. Similarly, we found the transient response near the source electrode. As shown in Fig. 6, both the amplitude of the change in channel conductivity and the speed of this change are faster near the drain electrode than they are near the source electrode. Furthermore, if we compare these responses to the electrical response, we see that optical response is significantly slower. To see if the results shown in Fig. 6 are part of a larger trend, we have plotted the time constant of the optical response at 30 pixel intervals along the OECT channel. In Fig. 7, we can see a clear trend of increasing time constant with increasing distance from the drain electrode.

4. DISCUSSION

As mentioned above, the results shown in Fig. 5 may follow a Poisson-Boltzmann model, and they are not terribly surprising. Because the drain voltage is negative with respect to the source, there is a stronger field between the gate and drain than there is between the gate and source. This larger field near the drain tends to push more sodium ions toward the drain, thus reducing its conductivity more noticeably than that near the source. While the results in Fig. 5 confirmed our existing expectations, those shown in Fig. 7 did not follow existing models. In particular, according to the Bernards and Malliaras model, we'd expect the time constant for the conductivity change to be given by the RC time constant of the ionic circuit linking the gate and OECT channel[9]. However, due to the geometric symmetry of the OECT, we'd expect the RC time constant to be the same at the drain as it is at the source, yet this is not what we observe. One reason for this departure from the expected behavior might be that the capacitance between the OECT channel and the gate electrode is voltage dependent. Because this capacitance arises from electrolytic double layer capacitances, such a voltage dependence would agree with existing models[21]. Another peculiar result found in our work is the fact that the electrical time constant is shorter than any of the measured optical time constants. One possible explanation for this is that the electrical response is dominated by a small region immediately adjacent to the drain electrode. If dedoping happens very quickly there, a depletion region can form in series with the rest of the OECT channel and greatly decrease the overall channel conductance. With the existing experimental setup, we are not able to monitor the optical response within a few micrometers of the electrodes because of shading and diffraction around the electrode edges. In future

Downloaded From: https://www.spiedigitallibrary.org/conference-proceedings-of-spie on 6/16/2018 Terms of Use: https://www.spiedigitallibrary.org/terms-of-use

studies, we will work to overcome these limitations in order to measure the response of the regions closest to the electrodes.

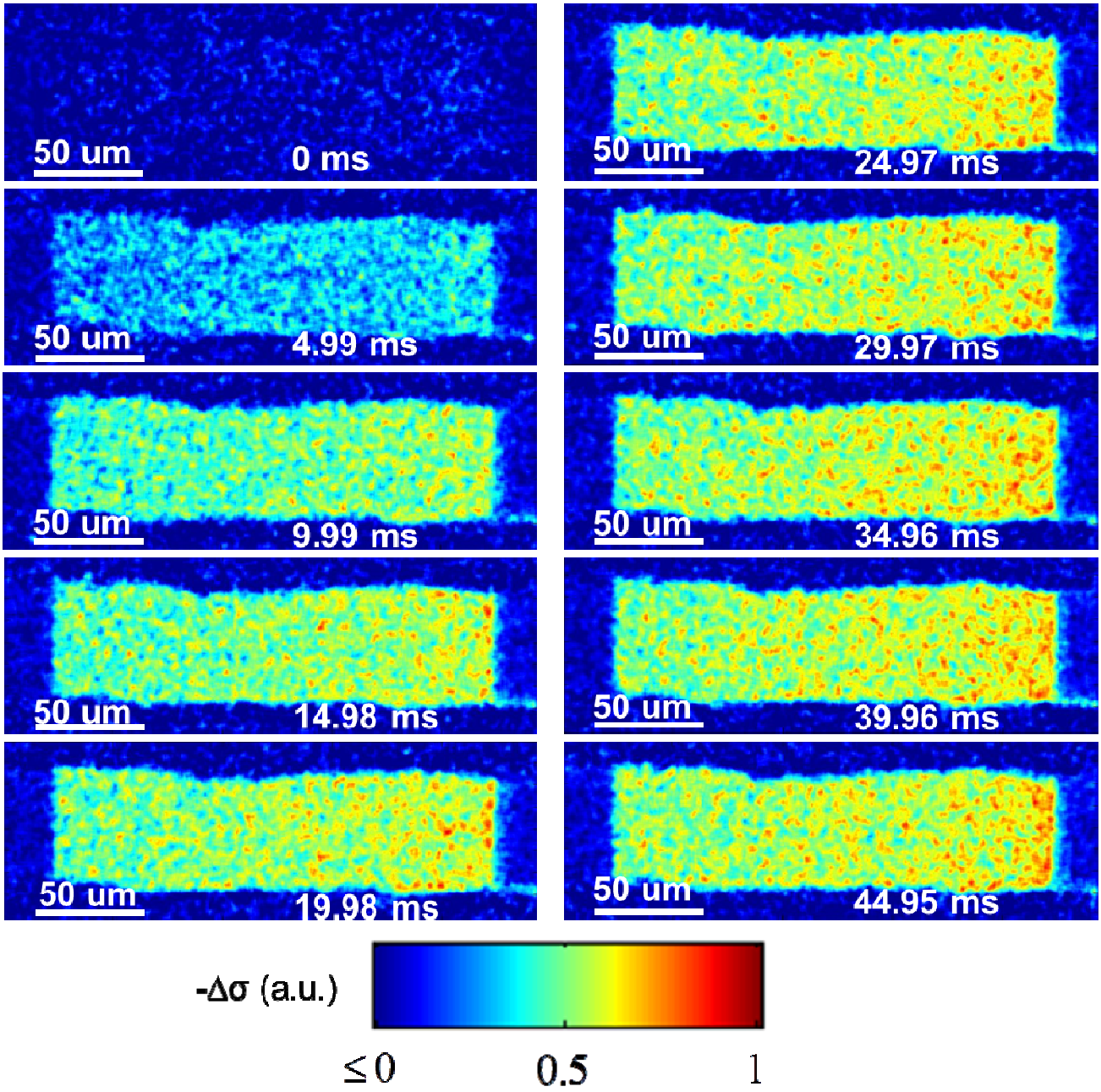

Figure 4. From top to bottom and left to right, a series of images showing the conductivity decrease after the gate voltage is stepped to 300 mV. In all frames, the source and drain electrodes are a 0 V and -300 mV, respectively. In the upper left frame the gate electrode is at 0 V, but in all other frames it is at 300 mV. Higher values on the color scale correspond to larger differences in pixel intensity after subtracting from the baseline image. (All electrodes are floating in the baseline image.)

Downloaded From: https://www.spiedigitallibrary.org/conference-proceedings-of-spie on 6/16/2018 Terms of Use: https://www.spiedigitallibrary.org/terms-of-use

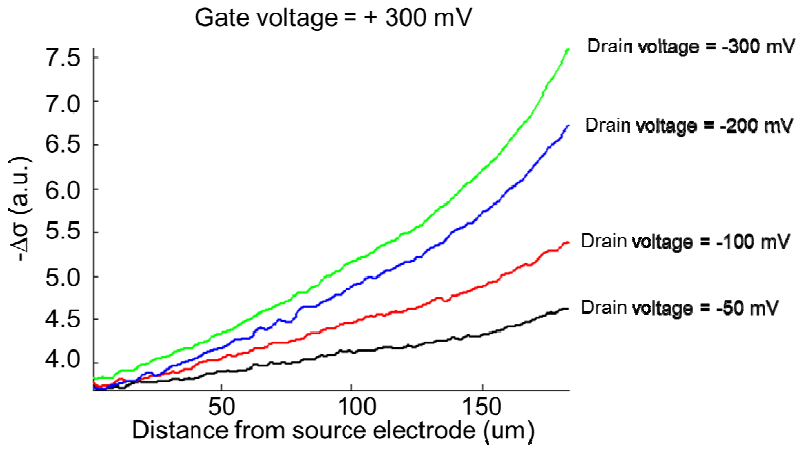

Figure 5. Conductivity profiles along the OECT channel. The conductivity change is measured by subtracting the steady state intensity profiles (after stepping the gate voltage) from the intensity profile of the initial image (with all electrodes floating). The two-dimensional intensity maps are reduced to one-dimensional profiles by averaging along pixel columns in the captured images.

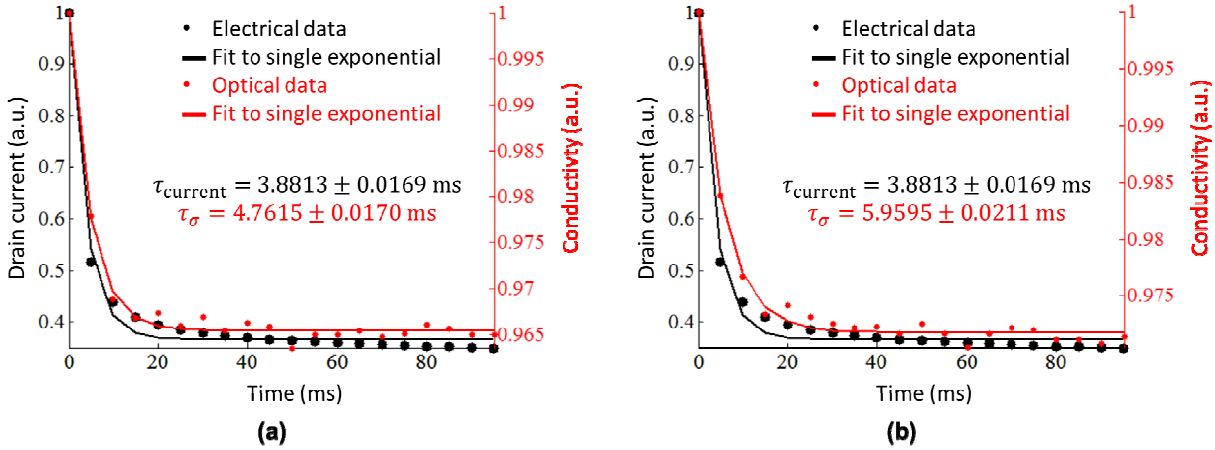

Figure 6. (a) The time response of the conductivity decrease near the drain electrode. (b) The time response of the conductivity decrease near the source electrode. Data, axes, and fits shown in red correspond to optical measurements while those shown in black correspond to electrical measurements.

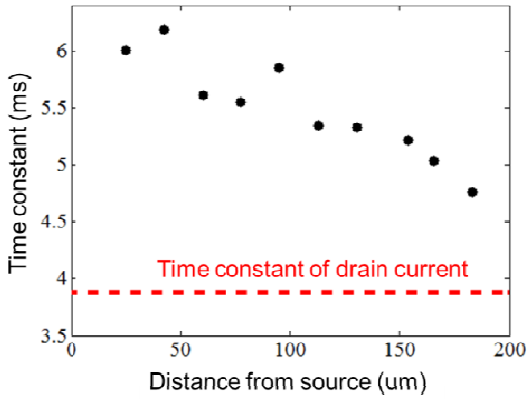

Figure 7. Time constants of optical response at different locations along the OECT channel.

Downloaded From: https://www.spiedigitallibrary.org/conference-proceedings-of-spie on 6/16/2018 Terms of Use: https://www.spiedigitallibrary.org/terms-of-use

5. CONCLUSION

In conclusion, we have demonstrated a novel method for characterizing OECTs. We have shown that we can use spatially and temporally resolved optical measurements to obtain conductivity profiles along the OECT channel and that the conductivity change occurs faster near the source than it does near the drain. Although we have not associated our results with a quantitative model, we have shown the utility of using these methods. Ultimately, these methods will be an important tool in improving our existing understanding of OECTs because they provide data that cannot be obtained via electrical measurements alone, and they will help inform an improved model of the transient response in OECTs.

Acknowledgements:

The authors would like to acknowledge funding from the U.S. Dept. of Education Graduate Assistantships in Areas of National Need (P200A120063) and U.S. National Science Foundation Career Award (ECCS 0847390).

REFERENCES

[1] Isaksson, J., Kjäl, P., Nilsson, D., Robinson, N., Berggren, M. and Richter-Dahlfors, A., "Electronic control of Ca^{2+} signalling in neuronal cells using an organic electronic ion pump," Nature Materials 6(9), 673-679 (2007).

[2] Khodagholy, D., Rivnay, J., Sessolo, M., Gurfinkel, M., Leleux, P., Jimison, L. H., Stavrinidou, E., Herve, T., Sanaur, S., Owens, R. M. and Malliaras, G. G., "High transconductance organic electrochemical transistors," Nature Communications 4, 2133 (2013).

[3] Jimison, L. H., Tria, S. A., Khodagholy, D., Gurfinkel, M., Lanzarini, E., Hama, A., Malliaras, G. G. and Owens, R. M., "Measurement of barrier tissue integrity with an organic electrochemical transistor," Advanced Materials 24(44), 5919-5923 (2012).

[4] Lin, P., Luo, X., Hsing, I. and Yan, F., "Organic electrochemical transistors integrated in flexible microfluidic systems and used for label-free DNA sensing," Advanced Materials 23(35), 4035-4040 (2011).

[5] Kergoat, L., Piro, B., Simon, D. T., Pham, M. C., Noël, V. and Berggren, M., "Detection of glutamate and acetylcholine with organic electrochemical transistors based on conducting polymer/platinum nanoparticle composites," Advanced Materials 26(32), 5658-5664 (2014).

[6] Campana, A., Cramer, T., Simon, D. T., Berggren, M. and Biscarini, F., "Organic electrochemical transistors: electrocardiographic recording with conformable organic electrochemical transistor fabricated on resorbable bioscaffold," Advanced Materials 26(23), 3873-3873 (2014).

[7] Khodagholy, D., Doublet, T., Quilichini, P., Gurfinkel, M., Leleux, P., Ghestem, A., Ismailova, E., Herve, T., Sanaur, S., Bernard, C. and Malliaras, G. G., "In vivo recordings of brain activity using organic transistors," Nature Communications 4, 1575 (2013).

[8] Kim, Y. H., Sachse, C., Machala, M. L., May, C., Müller-Meskamp, L. and Leo, K., "Highly conductive PEDOT: PSS electrode with optimized solvent and thermal post-treatment for ITO-free organic solar cells," Advanced Functional Materials 21(6), 1076-1081 (2011).

[9] Bernards, D. A. and Malliaras, G. G., "Steady-state and transient behavior of organic electrochemical transistors," Advanced Functional Materials 17(17), 3538-3544 (2007).

[10] Khodagholy, D., Gurfinkel, M., Stavrinidou, E., Leleux, P., Herve, T., Sanaur, S. and Malliaras, G. G., "High speed and high density organic electrochemical transistor arrays," Applied Physics Letters 99(16), 163304 (2011).

[11] Zhang, M., Lin, P., Yang, M. and Yan, F., "Fabrication of organic electrochemical transistor arrays for biosensing," Biochimica et Biophysica Acta-General Subjects 1830(9), 4402-4406 (2013).

[12] Herlogsson, L., Noh, Y. Y., Zhao, N., Crispin, X., Sirringhaus, H. and Berggren, M., "Downscaling of organic field-effect transistors with a polyelectrolyte gate insulator," Advanced Materials 20(24), 4708-4713 (2008).

[13] Huang, J. H., Kekuda, D., Chu, C. W. and Ho, K. C., "Electrochemical characterization of the solvent-enhanced conductivity of poly (3,4-ethylenedioxythiophene) and its application in polymer solar cells," Journal of Materials Chemistry 19(22), 3704-3712 (2009).

[14] Ouyang, J., Xu, Q., Chu, C. W., Yang, Y., Li, G. and Shinar, J., "On the mechanism of conductivity enhancement in poly (3,4-ethylenedioxythiophene): poly (styrene sulfonate) film through solvent treatment," Polymer 45(25), 8443-8450 (2004).

Downloaded From: https://www.spiedigitallibrary.org/conference-proceedings-of-spie on 6/16/2018 Terms of Use: https://www.spiedigitallibrary.org/terms-of-use

[15] Wang, X. and Smela, E., "Experimental studies of ion transport in PPy(DBS)," The Journal of Physical Chemistry C 113(1), 369-381 (2008).
[16] Stavrinidou, E., Leleux, P., Rajaona, H., Khodagholy, D., Rivnay, J., Lindau, M., Sanaur, S. and Malliaras, G. G., "Direct measurement of ion mobility in a conducting polymer," Advanced Materials 25(32), 4488-4493 (2013).
[17] Tarabella, G., Nanda, G., Villani, M., Coppedè, N., Mosca, R., Malliaras, G. G., Santato, C., Ianotta, S. and Cicoira, F., "Organic electrochemical transistors monitoring micelle formation," Chemical Science 3(12), 3432-3435 (2012).
[18] Xuan, Y., Sandberg, M., Berggren, M. and Crispin, X., "An all-polymer-air PEDOT battery," Organic Electronics 13(4), 632-637 (2012).
[19] Wang, X. and Smela, E., "Color and volume change in PPy(DBS)," The Journal of Physical Chemistry C 113(1), 359-368 (2008).
[20] Kirby, B.J., [Micro- and Nanoscale Fluid Mechanics], Cambridge University Press, New York, 199-206 (2010).
[21] Bazant, M. Z., Storey, B. D. and Kornyshev, A. A., "Double layer in ionic liquids: Overscreening versus crowding," Physical Review Letters 106(4), 046102 (2011).

Downloaded From: https://www.spiedigitallibrary.org/conference-proceedings-of-spie on 6/16/2018 Terms of Use: https://www.spiedigitallibrary.org/terms-of-use